

Chapter 12

Instability & Mass Loss near the Eddington Limit

S.P. Owocki and N.J. Shaviv

Abstract We review the physics of continuum-driven mass loss and its likely role in η Carinae and LBVs. Unlike a line-driven wind, which is inherently limited by self-shadowing, continuum driving can in principle lead to mass-loss rates up to the “photon-tiring” limit, for which the entire luminosity is expended in lifting the outflow. We discuss how instabilities near the Eddington limit give rise to a clumped atmosphere, and how the associated “porosity” can regulate a continuum-driven flow. We also summarize recent time-dependent simulations in which a mass flow stagnates because it exceeds the tiring limit, leading to complex time-dependent inflow and outflow regions. Porosity-regulated continuum driving in super-Eddington epochs can probably explain the large, near tiring-limit mass loss inferred for LBV giant eruptions. However, while these extreme flows can persist over dynamically long periods, they cannot be sustained for an evolutionary timescale; so ultimately it is stellar structure and evolution that sets the overall mass loss.

12.1 Introduction

LBV giant eruptions or “supernova imposters” are characterized by strongly enhanced luminosity and substantial mass ejection. An extreme example is η Carinae, which during its giant eruption of 1840–1860 ejected $10M_{\odot}$ or more at speeds of $300\text{--}800\text{ km s}^{-1}$, implying a kinetic energy rate comparable to the peak radiative

S.P. Owocki (✉)

Bartol Research Institute, Department of Physics & Astronomy, University of Delaware,
Newark, DE 19716 USA

e-mail: owocki@bartol.udel.edu

N.J. Shaviv

Racah Institute of Physics, Hebrew University, GivUat Ram, Jerusalem 91904 Israel

e-mail: shaviv@phys.huji.ac.il

luminosity $L \approx 20 \times 10^6 L_\odot$ seen during the eruption [12, 25, 43]. The total energy release is only a few percent of the 10^{51} erg non-neutrino output in a typical supernova, but represents a substantial fraction of the binding energy of the layers outside the star’s core. Such extreme mass loss is orders of magnitude greater than one expects in a standard CAK model for radiative driving by scattering in metal-ion lines [7].

The association of η Car and other LBVs with the empirical upper limit of luminosity for observed stars [23] has led to a general view that such strong episodes of mass loss may result from the star’s approach to the classical Eddington limit, at which the continuum radiative force due to Thomson scattering equals the inward force of gravity [1, 10, 24, 25]. Normally, if the radiative flux approaches the Eddington limit in a star’s interior, convection arises and carries enough of the energy flux to keep the interior sub-Eddington, as we explain in Sect. 12.2.3 below. On the other hand, no fundamental constraint prohibits the existence of a quasi-steady state with very high radiation fluxes in the outer layers of a star. As we show in Sect. 12.2.4, a super-Eddington luminosity may persist for a substantial length of time once we consider that high fluxes also give rise to instabilities.

This can lead to a situation analogous to classical novae, wherein the sudden onset of shell burning induces a super-Eddington brightness that lasts for several months; e.g., Nova LMC 1988 #1 was super-Eddington for about 50 days [36]. Since this is much longer than any dynamical timescale in the nova system, it can result in a quasi-steady wind mass loss, driven by continuum rather than line opacity. In fact, it was realized that optically thick continuum-driven winds explain many characteristics of these objects long before it was understood how super-Eddington luminosities could arise [3]. Unlike LBVs with poorly determined masses, novae have the Chandrasekhar mass as a strict upper limit, so there is no doubt that they are indeed super-Eddington [40].

Whatever mechanism may trigger such a super-Eddington brightening in LBVs, a key issue is how the continuum driving is regulated to keep the stellar interior gravitationally bound, while allowing a sustainable mass loss from near the surface. As discussed below, it seems that interior convection, flow stagnation, and the ‘porosity’ of a clumped medium may all play a role. A likely result is a mass loss rate that approaches the “photon-tiring limit”, associated with the finite energy available to lift material out of the star’s gravitational potential. This is several orders of magnitude higher than can be achieved by line-driving, and is indeed comparable to the mass loss rate, $\sim 1 M_\odot \text{year}^{-1}$, inferred for the giant eruption of η Carinae [33].

However, the associated mass loss time scale, $t_{\dot{M}} = M/\dot{M} \sim 100$ year, is so short that this state can only be sustained for a few years before inducing fundamental readjustments in the stellar structure. After the super-Eddington condition has thus been quenched, a much longer thermal timescale probably elapses before another outburst [25, 29]. But even with a limited duty cycle, such eruptions can dramatically reduce the star’s mass within its evolutionary timescale. Such LBV mass loss may play a central role in the evolution and final fate of the most massive stars, and may be a key factor in setting the stellar upper mass limit. Moreover, unlike CAK line-driving, these continuum-driven processes do not depend directly on

metallicity. Thus they may play a similar role in the first generation of massive stars (“Population III”), which are thought to have helped to reionize the universe following the recombination epoch of the Big Bang.

Below we elaborate on this role of radiation forces for both the interior structure (Sect. 12.2) and mass loss (Sect. 12.3) of massive stars. A concluding discussion (Sect. 12.4) considers general issues related to the energy source of the giant eruptions and various implications for massive star evolution near the Eddington limit.

12.2 Radiation Pressure in Massive Stars

The key to understanding the internal structure of massive stars is to recognize the effects that arise in the presence of very strong radiative flux. In Sect. 12.2.1 we begin by discussing the radiative force and the Eddington limit. In Sect. 12.2.2, we demonstrate how the radiative pressure changes the mass luminosity relation. In Sect. 12.2.3 we show that as the Eddington luminosity is approached, convection is necessarily excited, implying that the interior of a star never becomes super-Eddington. In Sect. 12.2.4 we discuss the instabilities that porosify the outer atmosphere. The combined effects allow us to build a coherent picture, in Sect. 12.2.5, for *quasi-static* structure in super-Eddington stars, such as η Car during its giant eruption.

12.2.1 Radiative Force and the Eddington Limit

Let us begin by considering the general form for the radiative acceleration \mathbf{g}_{rad} associated with opacity κ_ν (a.k.a. the mass absorption coefficient, with units $\text{cm}^2 \text{g}^{-1}$) in stellar material with a radiative flux \mathbf{F}_ν at photon frequency ν :

$$\mathbf{g}_{rad} = \int_0^\infty \frac{\kappa_\nu \mathbf{F}_\nu}{c} d\nu. \quad (12.1)$$

Here κ_ν includes continuum processes – Thomson scattering by electrons plus bound-free and free-free absorption – and bound-bound transitions.

In a static interior or atmosphere, where saturation of spectral lines keeps the associated line-force small, \mathbf{g}_{rad} is dominated by continuum processes, mainly Thomson scattering in the cases discussed here. Because Thomson opacity is gray (frequency-independent), it can be pulled outside the frequency integration in (12.1). In an idealized, spherically symmetric, radiative envelope, the bolometric flux $F = \int_0^\infty F_\nu d\nu$ is purely radial, $F = L/4\pi r^2$ where L is the bolometric luminosity. The radiative acceleration associated with a gray opacity κ is thus

$$g_{rad} = \frac{\kappa F}{c} = \frac{\kappa L}{4\pi r^2 c} \equiv \Gamma g. \quad (12.2)$$

Here Γ is the Eddington parameter L/L_{Edd} , where $L_{\text{Edd}} \equiv 4\pi GMc/\kappa$ and M is the stellar mass. This is the ratio of the radiative acceleration to the local gravitational acceleration $g = GM/r^2$. Since both gravity and radiative flux have the same r^{-2} dependence, Γ is almost independent of radius in regions where the gradients of κ , L , and M are small.¹ For the classical case of pure Thomson scattering and “normal” chemical composition, the Eddington parameter is quantitatively

$$\Gamma_e \approx 2.6 \times 10^{-5} \frac{(L/L_\odot)}{(M/M_\odot)}. \quad (12.3)$$

As discussed in the next subsection, stellar luminosity scales with a high power of the stellar mass, $L \propto M^3$, so hot massive stars with $M > 10M_\odot$ generally have $\Gamma_e > 0.1$, possibly even approaching unity. Indeed $\Gamma_e = 1$ defines the *classical Eddington limit* for the L/M ratio where an idealized star would become unbound.

It should be emphasized, however, that this does not represent an appropriate condition for normal steady mass loss, which requires an outwardly increasing radiative force that goes from being *less* than gravity inside the star to *exceeding* gravity in the outflowing wind. Section 12.3 summarizes how the necessary force modulation can occur through line-desaturation for line driving, and through porosity of spatial structure for continuum driving.

12.2.2 Stellar Structure Scaling for Luminosity vs. Mass

The interior structure of a star is set by the dual requirements for hydrostatic balance and energy transport. As Eddington found [14], we can use these to derive a simple scaling relation for stellar luminosity vs. mass. Let us begin with the classic formula for radiative flux F_{rad} via outward diffusion of radiation energy density U_{rad} ,

$$F_{\text{rad}} = -\frac{c}{3\kappa\rho} \frac{dU_{\text{rad}}}{dr}. \quad (12.4)$$

Since $P_{\text{rad}} = U_{\text{rad}}/3$, (12.4) can be rearranged to show that the gradient of radiation pressure is a radiative force per unit volume,

$$\frac{dP_{\text{rad}}}{dr} = -\frac{\kappa F_{\text{rad}}}{c} \rho = -g_{\text{rad}} \rho = -\Gamma g \rho = -\Gamma \frac{GM}{r^2} \rho. \quad (12.5)$$

Subtracting this from the hydrostatic equation that sets the gradient of total pressure $P = P_{\text{gas}} + P_{\text{rad}}$, we find that *gas* pressure in a static model satisfies

$$\frac{dP_{\text{gas}}}{dr} = -(1 - \Gamma) \frac{GM}{r^2} \rho. \quad (12.6)$$

¹As discussed below, there are various circumstances in which this is not the case.

Combined with mass conservation and the ideal gas law, (12.4) and (12.6) form the basis for Eddington's $n = 3$ polytrope model for stars with radiative interiors [14]. In such a model the Eddington parameter has a simple scaling with stellar mass,

$$\frac{\Gamma}{(1-\Gamma)^4} = \mu^4 \left(\frac{M}{18.3M_\odot} \right)^2 \approx \left(\frac{M}{48M_\odot} \right)^2, \quad (12.7)$$

where the molecular weight μ is approximately $4/(5X+3)$ in a fully ionized mix with hydrogen mass fraction X . The second equality in (12.7) applies for hydrogen abundance $X = 0.7$, $\mu \approx 0.62$.

This scaling can be understood from the average gradients in (12.4) and (12.6) in terms of stellar mass M and radius R . Using the ideal gas law $P_{gas} \sim \rho T$ with $\rho \sim M/R^3$, (12.6) implies that the characteristic interior temperature scales as

$$T \sim (1-\Gamma) \frac{M}{R}. \quad (12.8)$$

With the further proportionalities $F_{rad} \sim L/R^2$ and $U_{rad} \sim T^4$, (12.4) gives

$$L \sim \frac{R^4 T^4}{M}. \quad (12.9)$$

Combining (12.8) and (12.9), we can eliminate both R and T to find

$$L \sim (1-\Gamma)^4 M^3 \quad \text{or} \quad \frac{\Gamma}{(1-\Gamma)^4} \sim M^2, \quad (12.10)$$

which agrees with (12.7). Note that this result does not depend on the nature of energy generation in the stellar core.²

Figure 12.1 shows a log-log plot of the resulting variation of luminosity vs. mass. For $M \lesssim 20M_\odot$ it implies a strong $L \sim M^3$ scaling, but for higher masses the $1-\Gamma$ term acts as a strong repeller away from the Eddington limit, causing a bend toward a linear asymptotic scaling $L \sim M$.

Formally this scaling suggests it is possible to have stars with arbitrarily large mass, approaching arbitrarily close to the Eddington limit. But surveys of dense young clusters are providing evidence for a cutoff in the stellar mass distribution at about $M \approx 150 - 200 M_\odot$ [15, 28, 31, 52].³

²Of course these simple relations have to be modified to accommodate gradients in the molecular weight as a star evolves from the zero-age main sequence. Equation 12.10 fails entirely for cool giant and supergiant stars where convection dominates the energy transport, but such objects are beyond the scope of this review.

³[Editors' comment:] This has long been suspected on other grounds. For instance, if one extrapolates the empirical upper limit in the HR diagram to high temperatures, it approaches the ZAMS around $200 M_\odot$ [23–25]. Various clues seem to implicate the same mass range.

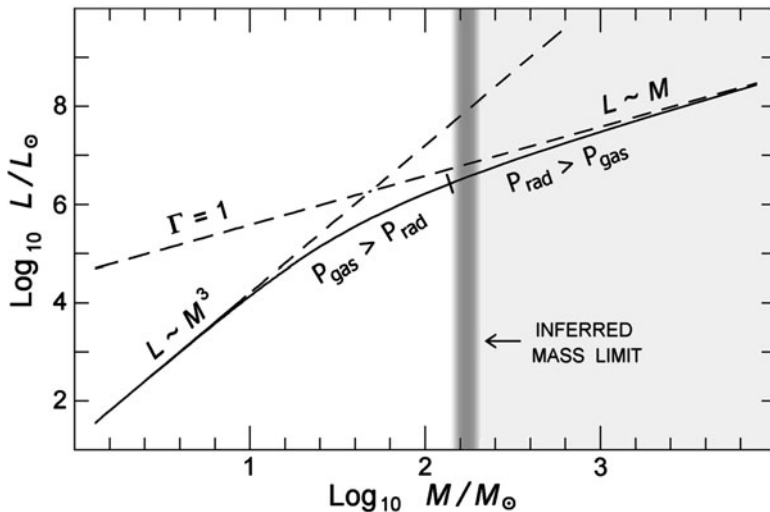


Fig. 12.1 Schematic log-log plot of stellar luminosity vs. mass for idealized $n = 3$ polytrope models, (12.7). For real stars the shape and normalization of the curve are somewhat altered by convection, variations in opacity and molecular weight, and other effects. The “inferred mass limit” at $150\text{--}200 M_{\odot}$ is based mainly on observations, not theory

In Fig. 12.1, this inferred upper mass limit is slightly to the right of the $\Gamma = 0.5$ point; therefore $P_{rad} > P_{gas}$ in the most massive stars (This is particularly true for η Car [12]). Dominance by radiation pressure is somewhat analogous to having a heavier fluid support a lighter one, and, as discussed in Sect. 12.2.4, such a configuration may be subject to various kinds of instabilities, leading to spatial clumping and/or LBV-like brightness variations [37–39, 48]. Resulting mass loss may play a key role in setting the stellar upper mass limit.

12.2.3 Convective Instability of a Super-Eddington Stellar Interior

If the energy flux locally exceeds the Eddington limit in a stellar interior, this usually does *not* initiate mass loss. Instead $\Gamma \gtrsim 1$ induces convective instability [27]. In the deep interior the gas density is large enough to carry most of the heat flux via convection, thus lowering the radiative flux so Γ_{rad} remains safely below unity.

This suggests that a super-Eddington outflow should originate in near-surface layers where convection becomes inefficient. Within “mixing length” formalism [22], the convective energy flux is roughly

$$F_{conv} \approx v_{conv} l \frac{dU_{gas}}{dr} \lesssim v_s H \frac{dP_{gas}}{dr} \approx \rho v_s^3, \quad (12.11)$$

apart from factors of order unity. Here v_{conv} , l , and U_{gas} are the convective velocity, mixing length, and gas thermal energy density. In an ideal gas $U \sim P_{gas} = \rho v_s^2$, where ρ and v_s are the gas density and sound speed. If we limit the convective velocity to the sound speed and the mixing length to the gas pressure scale height $H = P_{gas}/(dP_{gas}/dr)$, then the inequality in (12.11) sets an upper bound on the convective energy flux. Below the layers where this limit is breached, convection can carry nearly the full energy flux, $F_{conv} \approx F = L/4\pi r^2$. But above that radius the convective flux is limited by the decline in ρv_s^3 . This shortfall demands a compensating increase in the radiative flux and thus in the radiative Eddington parameter:

$$\Gamma_{rad} = \frac{\kappa F_{rad}}{gc} = \frac{\kappa(F - F_{conv})}{gc} \approx \frac{L - 4\pi r^2 \rho v_s^3}{L_{Edd}}. \quad (12.12)$$

Consider now the critical radius R_c where convective inefficiency leads to $\Gamma_{rad} > 1$. If we put the sonic radius for a wind outflow [29] at this location, then (12.12) implies an associated mass loss rate⁴

$$\dot{M}_{conv} \approx 4\pi R_c^2 \rho_c v_s \approx \frac{L - L_{Edd}}{v_s^2} \approx (4 M_\odot \text{ year}^{-1}) \left(\frac{\Gamma - 1}{\Gamma} \right) \frac{L_6}{T_5}, \quad (12.13)$$

where L_6 and T_5 denote $L/10^6 L_\odot$ and $T/10^5 \text{ K}$. In the near-surface layers where convection becomes inefficient, T_5 is of order unity and $v_s \sim 40 \text{ km s}^{-1}$.

For luminosities well above the Eddington limit, (12.13) gives an unsustainably high mass loss rate. The ‘‘photon tiring limit,’’ set by the energy required to lift material out of the star’s gravitational potential [32, 33], is

$$\dot{M}_{tir} \approx \frac{L}{v_{esc}^2/2} \approx \frac{L}{GM/R_c} \approx (0.032 M_\odot \text{ year}^{-1}) \frac{(R_c/R_\odot)}{(M/M_\odot)} L_6. \quad (12.14)$$

If $\Gamma \gtrsim 1.5$, $T_5 \sim 1$, and $M/R \sim M_\odot/R_\odot$, (12.13) predicts a mass loss rate that exceeds the tiring limit by a factor of order $(v_{esc}/v_s)^2 \sim 100$. This means that L cannot sustain a mass loss initiated near R_c ; the flow would stagnate at about $r \approx 1.01 R_c$ with the above parameters. In other words no consistent super-Eddington outflow can originate at the top of the region of efficient convection [38].

12.2.4 Radiative Instability and Porosification of Atmospheres

If we are to explain the super-Eddington episode in η -Car and other objects in terms of sustained outflow, the above analysis shows that the sonic radius R_s , where the net radial force vanishes, must be shifted outward to a layer whose mass density is much

⁴[Clarification:] In this review as in most discussions of stellar mass loss, \dot{M} denotes $|dM/dt|$ rather than the negative quantity dM/dt .

smaller than at the inefficient convection radius R_c . Thus the region $R_c < r < R_s$ must be quasi-hydrostatic with a declining density and pressure, even though $\Gamma_{rad} > 1$ traditionally implies a net outward force there!

The resolution to this paradox has two aspects. First, as an atmosphere approaches the Eddington luminosity, many possible instabilities can give rise to inhomogeneities. Second, optically thick inhomogeneities (“clumps”), reduce the effective opacity, thus allowing larger fluxes without increasing the radiative force.

Dating back to early work by Spiegel [46, 47], there have been speculations that atmospheres supported by radiation pressure would exhibit instabilities not unlike that of Rayleigh-Taylor, associated with the support of a heavy fluid by a lighter one, leading to formation of “photon bubbles”. Quantitative stability analyses [39, 48] show that even a simple case of a pure “Thomson atmosphere” – i.e., supported by Thomson scattering of radiation by free electrons – develops lateral inhomogeneities. The analysis by Shaviv [39] suggests that these instabilities share many of the properties of “strange mode” pulsations [18, 34]. They are favored when radiation pressure dominates over gas pressure, and occur when the temperature perturbation term becomes non-local. In strange mode instabilities, the relevant term arises because temperature in the diffusion limit depends on the radial gradient of the opacity perturbations. In the pure-Thompson lateral instability, the term depends on lateral radiative flux, which involves non-radial structure comparable in size to the scale height. More instabilities exist if the model is not a pure Thomson atmosphere; absorption opacity can induce the aforementioned strange modes, and magnetic fields imply additional phenomena [2, 4, 6, 16].⁵ The specific physical causes of these instabilities, however, are not fundamental to the discussion here. The two essential points are: (1) As atmospheres approach the Eddington limit, non-radial instabilities make them inhomogeneous on a horizontal scale comparable to the vertical scale height; and (2) Such inhomogeneities change the ratio between the radiative *flux* and the radiative *force*.

In the presence of inhomogeneities in density ρ , the outward radiation flux can be written as a volume average $\langle F \rangle_V$, while the force per unit volume that it exerts is $\langle F \kappa \rho \rangle_V / c$. Thus an “effective” opacity for the force can be defined as [37],

$$\kappa_{\text{eff}} \equiv \frac{\langle F \kappa \rho \rangle_V}{\langle F \rangle_V \langle \rho \rangle_V}. \quad (12.15)$$

(This is analogous to opacity variation in *frequency* space in non-gray atmospheres, wherein radiative force depends on a flux-weighted mean integrated over frequency instead of volume. The “Rosseland mean” defined in textbooks is pertinent.)

⁵[Editors’ comment:] One should also recall the “modified Eddington limit” often proposed in the 1980s for LBVs and η Car; see [1, 10, 24] and especially Sect. 5 in [25]. This is a hypothetical instability, based on temperature dependence of absorption opacity added to Thomson scattering in an 8,000–30,000 K atmosphere with $0.7 < \Gamma_e < 1$. Whether correct or not (which so far as we know has never been carefully tested), the MEL was a conceptual predecessor of some ideas outlined in this chapter; for instance it would obviously entail 3-D spatial inhomogeneities.

For some opacity laws, spatial inhomogeneity can enhance the effective opacity defined above. More generally, however, as in the special case of Thomson scattering, κ_{eff} is reduced. A calculable example is the limit of small isotropic perturbations in an optically thick Thomson-scattering atmosphere with negligible gas heat capacity, such that $\nabla \cdot \mathbf{F} = 0$. This case approximates a hot atmosphere, but deep enough for the inhomogeneities to remain opaque. Then one finds [37]

$$\kappa_{\text{eff}} = \left[1 - \left(\frac{\mathcal{D} - 1}{\mathcal{D}} \right) \sigma^2 \right] \kappa_0, \quad (12.16)$$

where σ is the normalized standard deviation of ρ and \mathcal{D} is the number of relevant spatial dimensions. This result shows that inhomogeneities tend to reduce the effective opacity, but not in a one-dimensional system. In other words the porosity effect is intrinsically *non-radial* and tends to *decrease* the effective opacity.

Because the “porous” state depends on non-linear behavior of relevant instabilities, and, in particular, on the mechanism saturating them, there are currently no ab initio calculations predicting characteristics such as $\kappa_{\text{eff}}(\Gamma)$ in the nonlinear state. This will require elaborate radiative hydrodynamic simulations.

12.2.5 Quasi-Static Structure of Super-Eddington Stars

The effects described in the previous subsections combine to give an overall picture for how stars can surpass the Eddington limit but remain, in a sense, stable (Fig. 12.2).

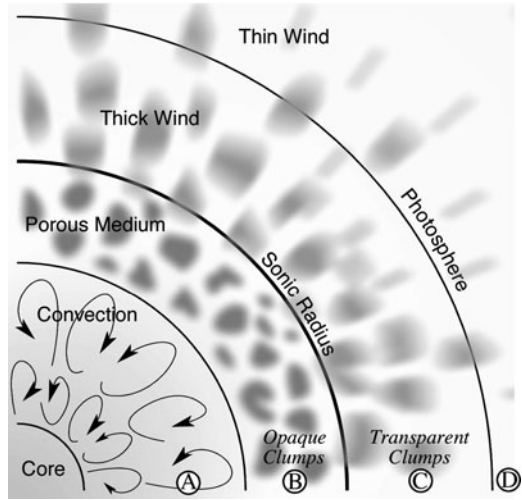
Region (A): As explained in Sect. 12.2.3, deep inside the star where the density is sufficiently high, excess flux above the Eddington luminosity is carried by convection. Thus we have a bound interior with $L_{\text{rad}} < L_{\text{Edd}} < L_{\text{tot}}$.

Region (B): Farther out where convection is inefficient, radiative instabilities cause the atmosphere to become inhomogeneous. This reduces the effective opacity and therefore increases the effective Eddington luminosity $L_{\text{Edd}}^{\text{eff}}$. This layer is bound, not because the radiation flux is lowered as in the convective region, but because the effective opacity is reduced: $L_{\text{Edd}} < L_{\text{rad}} < L_{\text{Edd}}^{\text{eff}}$.

Region (C): Farther out, each clump becomes transparent and the effective opacity returns to the microscopic value: $L_{\text{Edd}}^{\text{eff}} \approx L_{\text{Edd}}$. The resulting mass outflow has its sonic point where $L \approx L_{\text{Edd}}^{\text{eff}} \gtrsim L_{\text{Edd}}$. More about this in Sect. 12.3.

Region (D): Since the mass loss rate is large enough to be opaque, the photosphere resides in the wind itself [8, 25].

Fig. 12.2 The structure of a super-Eddington star from [41], see text (Sect. 12.2.5)



12.3 Radiatively Driven Mass Loss

12.3.1 Line-Driven Stellar Winds

As a basis for developing a model for continuum-driven mass loss from super-Eddington phases of LBV stars, let us review the more well-established theory for steady line-driven winds (For an account of stellar winds in general, see [29]).

The resonant nature of absorption in spectral lines leads to an opacity that is inherently much stronger than for free electrons. Comparing a bound electron to a free one, the enhancement in frequency-integrated cross-section can be represented as the “quality” value of the resonance, essentially the ratio of frequency to the damping frequency γ [17]. If we use a classical approximation for the latter,

$$Q \approx \frac{\nu}{\gamma} \approx \frac{3}{8\pi^2} \frac{\lambda}{r_e} \sim 10^7, \quad (12.17)$$

where λ is photon wavelength and $r_e = e^2/m_e c^2$ is the classical radius of the electron. Thus a bound electron typically scatters photons ten million times more effectively than a free electron does! Since only about 0.01% of the electrons in relevant layers of a hot star with typical metallicity are in bound states, the net enhancement is of the order of $\bar{Q} \sim 1,000$. In the idealized optically thin limit, the total spectral line force would exceed the Thomson-scattering force by a comparable factor [17]. For very massive stars one might therefore expect an enormous outward acceleration, $\bar{Q} \Gamma_e g \sim 1000g$.

In reality, of course, self-absorption in the lines prevents this from occurring. The effective optical depth in a mass flow is related to the local velocity gradient (the

Sobolev approximation [29, 45]). For a single line with frequency-averaged opacity $\kappa_q = q\kappa_e$, the acceleration factor $q\Gamma_e$ is reduced to

$$\Gamma_{\text{line}} \approx \left[\frac{1 - \exp(-qt)}{qt} \right] q\Gamma_e, \quad (12.18)$$

where $t = \kappa_e \rho c / (dv/dr)$ is the Sobolev optical depth of a line with unit strength $q = 1$ [7, 45]. In CAK line-driven wind theory, the number distribution of spectral lines vs. line-strength is approximated as a power law, $dN/dq \sim (q/\bar{Q})^{\alpha-1}$ with index α in the range 0.5–0.7. The associated total radiation force factor is then

$$\Gamma_{\text{lines}} = \frac{\bar{Q}\Gamma_e}{(1-\alpha)(\bar{Q}t)^\alpha} \propto \left(\frac{1}{\rho} \frac{dv}{dr} \right)^\alpha. \quad (12.19)$$

The latter proportionality emphasizes the scaling of the line-force with the velocity gradient and the *inverse* of the mass density. This keeps the line acceleration less than gravity in the dense, nearly static atmosphere, but also allows its outward increase to drive the outflowing wind.

The CAK mass loss rate is set by the associated critical density at which the outward line acceleration is just sufficient to overcome the gravity reduced by Thomson scattering, i.e., $\Gamma_{\text{lines}} \approx 1 - \Gamma_e$:

$$\dot{M}_{\text{CAK}} = \left(\frac{\alpha}{1-\alpha} \right) \left[\frac{\bar{Q}\Gamma_e}{1-\Gamma_e} \right]^{-1+1/\alpha} \frac{L}{c^2}. \quad (12.20)$$

Here we have used the fact that $v dv/dr \approx (1 - \Gamma_e)g$ in this type of solution. The same property implies the CAK velocity law $v(r) \approx (1 - R/r)^{1/2} v_\infty$, with the wind terminal speed being proportional to the effective surface escape speed,

$$v_\infty \propto v_{\text{esc}} \approx \left[(1 - \Gamma_e) \frac{GM}{R} \right]^{1/2}. \quad (12.21)$$

As a star approaches the classical Eddington limit $\Gamma_e \rightarrow 1$, these standard CAK scalings formally predict the mass loss rate to diverge as $\dot{M} \propto 1/(1 - \Gamma_e)^{(1-\alpha)/\alpha}$, but with a vanishing terminal flow speed $v_\infty \propto \sqrt{1 - \Gamma_e}$. The former might appear to provide an explanation for the large mass losses inferred in LBV's, but the latter fails to explain the moderately high inferred ejection speeds, e.g. the 500–800 km/s kinematic expansion inferred for the Homunculus nebula of η Carinae [12, 13, 43, 44].

So one essential point is that line-driving cannot explain the extremely large mass loss rates needed to explain the Homunculus nebula. To maintain the moderately high terminal speeds, the $\Gamma_e/(1 - \Gamma_e)$ factor would have to be of order unity. Then, with optimal realistic values $\alpha = 1/2$ and $\bar{Q} \approx 2,000$ for the line opacity parameters [17], the maximum mass loss due to line driving is [42]

$$\dot{M}_{\text{max,lines}} \approx 1.4 \times 10^{-4} L_6 M_\odot \text{ year}^{-1}, \quad (12.22)$$

where $L_6 = L/10^6 L_\odot$. Even for peak luminosities of a few times $10^7 L_\odot$ during η Car's great eruption, this limit is several orders of magnitude below the rate needed to form the Homunculus. Therefore, if mass loss in that event occurred via a wind, it must have been driven chiefly by continuum radiation force rather than lines [5, 35].

12.3.2 Continuum-Driven Winds Regulated by Porous Opacity

As discussed in Sect. 12.2.4, stars that approach or exceed the Eddington limit are expected to have complex spatial structure, and this has led to a new “porosity” paradigm [37, 38] for quasi-steady continuum driving from super-Eddington stars. As we now describe, the basic formalism can be cast in terms that draw heavily on the above theory for wind driving by line-opacity [33].

To begin, consider a medium in which material has coagulated into discrete clumps of individual optical thickness $\tau_{cl} = \kappa \rho_b \ell$, where ℓ is the clump size, and the clump density is enhanced compared to the mean density of the medium by a volume filling factor $\zeta = \rho_b / \rho$. The effective opacity of this medium can then be approximated by a form like the scaling of force in a single line (cf. 12.18),

$$\kappa_{\text{eff}} \approx \left[\frac{1 - \exp(-\tau_{cl})}{\tau_{cl}} \right] \kappa \quad (12.23)$$

For optically thin clumps ($\tau_{cl} \ll 1$) this gives the usual microscopic opacity, $\kappa_{\text{eff}} \approx \kappa$; but in the optically thick limit ($\tau_{cl} \gg 1$) κ_{eff} is reduced by a factor of $1/\tau_{cl}$. In that case the overall effective opacity is roughly the clump cross section divided by the clump mass: $\kappa_{\text{eff}} \approx \kappa / \tau_{cl} \approx \ell^2 / m_{cl}$. The critical mean density at which each clump becomes optically thin is $\rho_o \approx 1/\kappa h$, where $h = \ell/\zeta$ is a characteristic “porosity length” parameter. The overall radiative acceleration would likewise be reduced by a factor that depends on the mean density.

More realistically, it seems likely that structure should occur with a range of compression strengths and length scales. Noting the similarity of the single-scale and single-line correction factors (12.18) and (12.23), let us draw upon an analogy with the power-law distribution of line-opacity in the standard CAK model of line-driven winds, and thereby consider a *power-law-porosity* model wherein the associated structure has a broad range of porosity length h . As detailed by [33], this leads to an effective Eddington parameter that scales as

$$\Gamma_{\text{eff}} \approx \left(\frac{\rho_o}{\rho} \right)^{\alpha_p} \Gamma ; \quad \rho > \rho_o, \quad (12.24)$$

where α_p is a porosity power index analogous to the CAK line-distribution power index α , and $\rho_o = 1/\kappa h_o$, with h_o now the porosity-length associated with the strongest (i.e. most optically thick) clump.

In rough analogy with the convective mixing length [22] discussed in Sect. 12.2.3, let us further assume that h_o scales with gravitational scale height $H = v_s^2/g$. Then the requirement that $\Gamma_{\text{eff}} = 1$ at the wind sonic point yields a mass loss rate scaling with luminosity. For the canonical case $\alpha_p = 1/2$, this takes the form [33]

$$\dot{M}_{\text{por}} \approx 4 (\Gamma - 1) \left(\frac{L}{v_s c} \right) \left(\frac{H}{h_o} \right) \quad (12.25)$$

$$\approx 0.004 (\Gamma - 1) \frac{(L/10^6 L_\odot)}{(v_s/20 \text{ km s}^{-1})} \left(\frac{H}{h} \right) M_\odot \text{ year}^{-1}. \quad (12.26)$$

Comparison with the CAK scaling (12.20) for a line-driven wind shows that the mass loss can be substantially higher from a super-Eddington star with porosity-regulated, continuum driving. Applying the extreme luminosity $L \approx 2 \times 10^7 L_\odot$ estimated for the η Car's 1840–1860 outburst, which implies an Eddington parameter $\Gamma \sim 5$, the derived mass loss rate for a canonical porosity length $h_o = H$ is $\dot{M}_{\text{por}} \approx 0.3 M_\odot \text{ year}^{-1}$, quite comparable to the likely average during that epoch.

Overall, it seems that, together with the ability to drive fast outflow speeds (of order the surface escape speed), the porosity formalism offers a basis for self-consistent dynamical modeling of even the most extreme LBV outbursts, which, like the giant eruption of η Carinae, approach the photon tiring limit.

12.3.3 Photon Tiring in a Simple Super-Eddington Wind Model

Before discussing simulations of porosity models with base mass flux above the tiring limit, let us first examine analytic models of photon tiring for continuum-driven winds in which the Eddington factor is assumed to have an explicit spatial dependence $\Gamma(r)$. Specifically, let us assume that it increases outward from $\Gamma(r) < 1$ in a static interior, crossing unity at some radius R_s which represents the sonic point of a mass outflow. The density ρ_s and sound speed v_s at this point set the mass loss rate $\dot{M} = 4\pi R_s^2 \rho_s v_s$, but otherwise gas pressure has negligible effect on the further supersonic acceleration. The steady-state equation of motion thus reduces to

$$v \frac{dv}{dr} \approx -\frac{[1 - \Gamma(r)] GM}{r^2}; \quad r \gtrsim R_s. \quad (12.27)$$

Unlike the porosity models above, this equation of motion has no explicit dependence on density; so the resulting velocity law $v(r)$ would not depend on the amount of mass accelerated. More realistically, a given radiative luminosity can only produce a limited mass loss rate before the energy expended in accelerating the outflow against gravity requires a notable reduction in the radiative energy flux

itself. To take account of this “photon tiring,” we reduce the radiative luminosity according to the kinetic and potential energy of the flow:

$$L_{\text{reduced}}(r) = L_* - \left[\frac{v^2}{2} + \frac{GM}{R_s} - \frac{GM}{r} \right] \dot{M}. \quad (12.28)$$

Here L_* and M are practically the star’s total energy outflow and mass. (The assumed r -dependence of Γ is due to a gradient in $\kappa_{\text{eff}} L_{\text{reduced}}$). Defining scaled variables

$$w = \frac{v^2}{(2GM/R_s)} \quad \text{and} \quad x = 1 - \frac{R_s}{r}, \quad (12.29)$$

we find a dimensionless equation of motion with photon tiring:

$$\frac{dw}{dx} = -1 + [1 - m(w+x)] \Gamma(x). \quad (12.30)$$

Parameter m is the “tiring number,”

$$m = \frac{GM\dot{M}}{R_s L_*}, \quad (12.31)$$

which is the fraction of radiative energy expended in lifting the wind out of the stellar gravitational potential. Using integrating factors, one can obtain an explicit solution in terms of the integral quantity $\Lambda(x) = \int_0^x dx' \Gamma(x')$:

$$w(x) = -x + \frac{1}{m} \left[1 - e^{-m\Lambda(x)} \right] + w(0) e^{-m\Lambda(x)}, \quad (12.32)$$

where for typical hot-star atmospheres the sonic point boundary value is very small, $w(0) = v_s^2 R_s / 2GM < 10^{-3}$.

As a simple example, consider the form $\Gamma(x) = 1 + 0.1\sqrt{x}$. Figure 12.3 plots solutions $w(x)$ vs. x for various m . If m is small, the flow reaches a finite speed at large radii ($x \rightarrow 1$); but for larger m it eventually decelerates, stopping at some finite stagnation point x_{stag} where $w(x_{\text{stag}}) = 0$. The latter solutions represent flows in which the mass loss rate is too high for the given luminosity to lift the material to full escape at large radii. By considering the critical case where $w = 0$ at $x = 1$, we can define a maximum mass loss rate, given according to (12.32) by the relation

$$m_{\text{max}} = 1 - \exp[-m_{\text{max}}\Lambda(1)]. \quad (12.33)$$

Note that $\Lambda(1)$ is the average of $\Gamma(x)$ in the range $0 \leq x \leq 1$. A simple approximation accurate to about 10% in this range is $m_{\text{max}} \approx 1 - \exp[2 - 2\Lambda(1)]$.

Regardless of how large $\Lambda(1)$ becomes, it is always true that $m_{\text{max}} < 1$. By comparison, the maximum mass loss allowed by convective inefficiency (12.13)

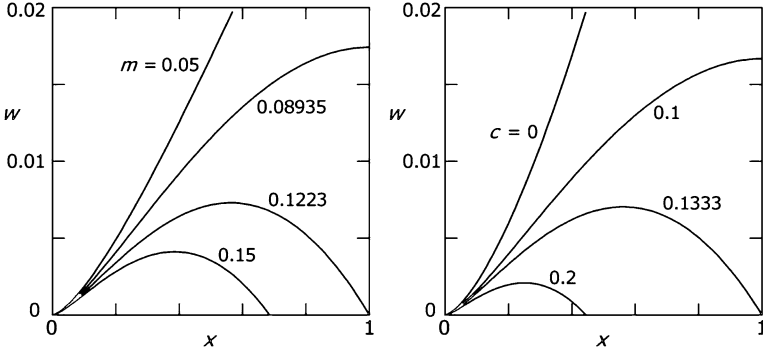


Fig. 12.3 Scaled kinetic energy w vs. radial parameter x for simple continuum-driven wind models, illustrating flow stagnation due to photon tiring (*left*) or to a post-peak decline of opacity (*right*). The curves are labeled with the photon tiring number m or opacity peak parameter c , see text

would correspond to a tiring number of order $m_{conv} \approx GM/R_s v_s^2 \approx 2v_{esc}^2/v_s^2$. Since typically $m_{conv} \gg 1$, we again see that any super-Eddington outflow initiated near the layer where convection becomes inefficient would stagnate by photon tiring.

In the limit of negligible tiring $m \ll 1$, solution (12.32) becomes $w(x) \approx \Lambda(x) - x$. Then the critical case of marginal escape, $w(1) = 0$, requires $\Lambda(1) = 1$. The right-hand part of Fig. 12.3 illustrates solutions for the specific nonmonotonic example $\Gamma(x) = 1 + 0.1\sqrt{x} - cx$, where c represents a tendency for κ_{eff} to decrease at large radii. For all $\Lambda(1) < 1$ (i.e., $c > 0.1333$), stagnation occurs at the radius where $\Lambda(x) = x$, precluding a steady flow. In a time-dependent model, material might accumulate there and then fall back to the star. This represents another way in which, instead of steady outflow, a super-Eddington region may give rise to an extended envelope with a 3-dimensional mass circulation and possibly a density inversion.⁶

12.3.4 Simulation of Stagnation and Fallback Above the Tiring Limit

For porosity models in which the mass flux exceeds the photon tiring limit, recent numerical simulations have explored the resulting complex pattern of infall and outflow [50, 51]. Despite the likely 3-D nature of such flow patterns, in order to keep the computation tractable this initial exploration assumes 1-D spherical symmetry, though allowing time-dependent density and flow speed. The total rate

⁶[Editors' comment:] In somewhat cooler hypergiant winds where other processes supplement radiative driving, phase changes from ionized to non-ionized hydrogen may produce interesting effects in unsteady outflows that resemble the case mentioned here. See, e.g., [26].

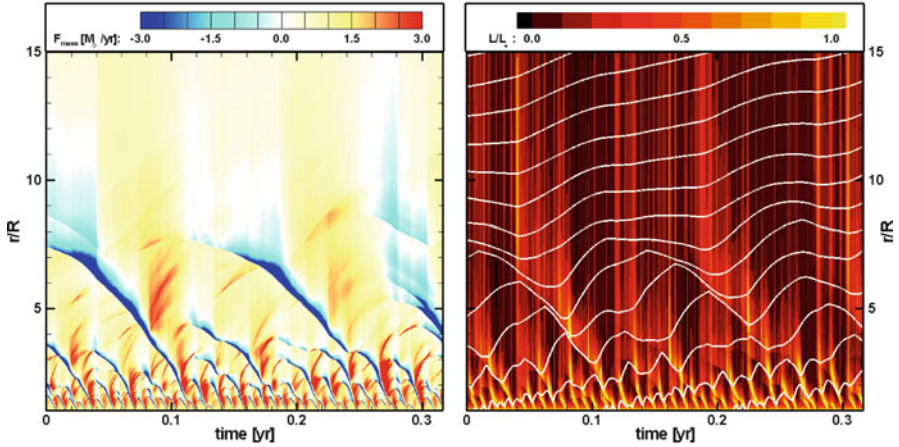


Fig. 12.4 Grayscale plot of radius and time variation of mass flux (*left*) and luminosity (*right*) in a time-dependent 1-D simulation of a super-Eddington wind with a porosity-mediated base mass flux which exceeds the photon tiring limit. The white contours on the right trace the height progression of fixed mass shells

of work done by the radiation on the outflow (or vice versa in regions of inflow) is again accounted for by a radial dependence of the radiative luminosity,

$$\frac{dL}{dr} = -\dot{m} g_{\text{rad}} = -\frac{\kappa_{\text{eff}} \rho v L}{c}, \quad (12.34)$$

where $\dot{m}(r,t) = 4\pi\rho v r^2$ is the varying local mass flux. The second equality follows from the definition (12.1) of radiative acceleration g_{rad} with a gray opacity κ_{eff} , set here by porosity-modified Thomson scattering. At each time step, (12.34) is integrated from an assumed lower boundary luminosity $L(R)$ to give the local radiative luminosity $L(r)$ at all radii $r > R$. Using this to compute $g_{\text{rad}}(r,t)$, the time-dependent equations for mass and momentum conservation are evolved forward to obtain the variations of density $\rho(r,t)$ and flow speed $v(r,t)$. (For simplicity, the temperature is fixed at the stellar effective temperature.) The base Eddington parameter is assumed to be $\Gamma = 10$, and the analytic porosity mass flux is 2.3 times the tiring limit.

Figure 12.4 illustrates the flow structure as a function of radius and time long after the initial condition. The left panel shows the local mass flux, ranging from $3 M_{\odot} \text{ year}^{-1}$ inward (black) to $3 M_{\odot} \text{ year}^{-1}$ outward (white). In the right panel, shading represents the local luminosity in units of the base value $L(r)/L(R)$, ranging from zero (black) to one (white); in addition, superposed lines represent the radius and time variations of selected mass shells.

Both panels show the remarkably complex nature of the flow, with positive mass flux from the base overtaken by a hierarchy of infall structures from stagnated flow above. Re-energization of the radiative flux by this infall gives the overlying region an outward impulse. The shell tracks show that, once material reaches a

radius $r \approx 5R$, its infall episodes become increasingly longer and eventually it drifts outward. The overall result is a net time-averaged mass loss through the outer boundary. Its rate is very close to the photon-tiring limit, and the terminal flow speed $v_\infty \approx 50 \text{ km s}^{-1}$ is substantially below the gravitational escape speed $v_{\text{esc}} \approx 600 \text{ km s}^{-1}$.

Of course the structure in a more realistic 3-D model is likely to be even more complex, and may lead to a highly porous medium. But it seems that one property of a super-Eddington star may be a mass loss rate comparable to the photon tiring limit.

12.4 Discussion

12.4.1 *LBV Eruptions: Enhanced Winds or Explosions?*

A key theme of this book is that extreme LBV eruptions can be “supernova imposters”, characterized by substantial brightening and large mass ejections. In this chapter we have modeled this mass loss in terms of a quasi-steady, continuum-driven wind that results when luminosity exceeds the Eddington limit. But an alternative paradigm is that such eruptions might be interior explosions that did not have sufficient energy to completely disrupt the star.

The overpressure from an explosion propagates through the star on a very short dynamical time scale, of order R/v_s where v_s is now the sound speed in very high-temperature gas heated by energy deposition of the explosion. In supernovae this sound speed is on the order of the mass ejection speed, $\sim 10,000 \text{ km s}^{-1}$. Even in a “failed” explosion it would be on the order of the surface escape speed, \sim a few hundred km s^{-1} , implying a dynamical time like the free fall time: a few days or less. The initial release of radiative energy results from expansion and peaks on a somewhat longer timescale of days or weeks for supernovae. (SN radioactive beta-decay becomes important in the later stages.) It is difficult to see how such a direct pressure-driven explosion can persist for years as seen in LBV eruptions.

This then is perhaps the key argument for a radiation-driven model. If energy is released in the deep interior, its *radiative* signature can take up to a much longer diffusion time to reach the surface.⁷ This can be long as a few years.

In contrast to the explosive disruption of supernovae, the total energy in an LBV eruption is well below the total stellar binding energy. Thus even if this energy were released suddenly in the deep interior, the initial dynamical response would quickly stagnate, leaving radiative diffusion as the substitute transport process. The associated excess luminosity may push the object over the Eddington limit, leading

⁷Since the luminous stars are likely to be mostly convective (Sect. 12.2.3), the limiting time scale is that of the convective diffusion mixing length time in the stellar core, which due to the high density is much longer than the dynamical time scale.

to strong, *radiatively driven* mass loss. Because the diffusion time scale is much longer than any dynamical time, the essential processes can be modeled as a quasi-steady continuum-driven wind as described above.

12.4.2 *Trigger & Energy Source for Super-Eddington Luminosity*

In a supernova the energy source is core-collapse to a neutron star or black hole. But in a giant LBV eruption, the post-eruption survival of an intact star, and indications that some LBVs can undergo multiple events of this type, show that the energy source cannot be a one-time singular event. Some other mechanism must provide the energy.

The total energy associated with an extreme eruption, mainly radiative luminosity and mechanical (i.e., kinetic and potential) energy in the wind, is a few times 10^{49} erg. For an eruption lasting a few decades, this corresponds to a power output of order $10^7 L_{\odot}$, which is only a few times the Eddington luminosity. This suggests that energy for the eruption can be supplied by the nuclear burning itself. If during quiescence the star shines at nearly the Eddington luminosity, a 10% increase in the central temperature would allow the CNO cycle or other reactions to supply the extra energy. Two implications follow.

First, the change in the binding energy required to get the increased temperature is only 10% of the binding energy of an $n = 3$ polytrope. Taking a mass $M \sim 100 M_{\odot}$ and radius $R \sim 100 R_{\odot}$, the energy change is $\sim 0.1 \Gamma GM^2 / (2R) \sim 10^{49}$ ergs. In other words, the energy associated with the eruption is comparable to the change in binding energy needed in order to supply the extra energy through nuclear reactions. This implies that the whole star can participate in the eruption.

Second, because the energy for the eruption can be continuously generated, many different scenarios can be envisioned for the triggering mechanism. Moreover, an instability originating in the outer layers, which then forces the interior to progressively adjust downward in the manner of a geyser [9,25], may be as favorable as a mechanism that originates in the core. Thus quite a few mechanisms have been suggested to explain LBV eruptions. Here are several examples.

In a linear analysis of radial modes using standard opacity tables, Glatzel and Kiriakidis found mode-coupling instabilities in the outer layers of massive stars [19]. Guzik et al. then showed how such an instability can propagate inward as convection arises [21]. Since convection takes a finite time to adjust, a super-Eddington luminosity can arise, with consequent ejection of mass.

Other instabilities originating in stellar envelopes were found by Stothers and Chin [49], who conjectured that η Car is repeatedly encountering ionization-induced dynamical instability, and by Maeder [30], who found that super-Eddington layers may occur somewhat deeper in.⁸

⁸[Editors' comment:] An older idea also seems pertinent here, see footnote in Sect. 12.2.4.

As a contrast, other instabilities could originate at the core. Guzik [20], for example, suggested that nonradial gravity mode oscillations grow slowly to an amplitude sufficient to cause an episode of mixing of hydrogen-rich material downward into hotter denser layers, which would generate a burst of nuclear energy release. Most recently, Woosley et al. [53] have emphasized the potential role of pulsational pair instability in the stellar core for powering either supernovae or giant LBV eruptions.

Because luminous stars have large radiative pressure support, their outer regions tend to be loosely bound and so exhibit various instabilities. This explains the plethora of suggested mechanisms. Unfortunately, however, none seems markedly better than the others.

It is yet unclear why LBVs erupt, and what sets the eruption time scale, the total ejected mass, or what determines the eruption repetition rate. *There is currently no model which predicts these numbers.*

12.4.3 Evolution near the Eddington Limit

The evolution of extremely massive stars is not yet understood. In particular, the potentially key evolutionary role of continuum-driven mass loss has only recently begun to be fully appreciated, and the super-Eddington conditions driving this mass loss depend on instabilities that are still quite poorly understood.

Nevertheless, because the mass loss rates associated with super-Eddington states are so extremely large, it is possible to discuss the average state of these objects without relying on details. Such huge mass loss rates simply cannot be sustained over the evolutionary time scales. Thus, once a star reaches a near-Eddington state, it must evolve without crossing the Eddington limit for too long, since the large mass loss serves as a negative feedback to reduce the luminosity of the star.

To see this behavior more quantitatively, we can again apply the Eddington $n = 3$ polytrope model discussed in Sect. 12.2.2, particularly the scaling for Γ in terms of stellar mass M and “molecular weight” μ . Recall (12.7):

$$\frac{\Gamma}{(1-\Gamma)^4} = \mu^4 \left(\frac{M}{18.3M_{\odot}} \right)^2,$$

where $\mu = 1/(2 - 5Y/4)$ for a mix of ionized hydrogen and helium with helium mass fraction Y . As the star evolves, its μ increases. If the mass loss rates are small (e.g., in a line-driven wind), M remains nearly constant so the increase in μ forces an increase in Γ . Without the effect of porosity, this would cause the star to approach the Eddington luminosity without actually reaching it.

However, once Γ exceeds some critical value, instabilities can make the atmosphere porous and allow a super-Eddington flux which implies a continuum-driven wind. According to (12.26), this mass loss would evaporate the star on a time scale much shorter than its several-million-year lifetime, unless $(\Gamma - 1) \ll 0.1$.

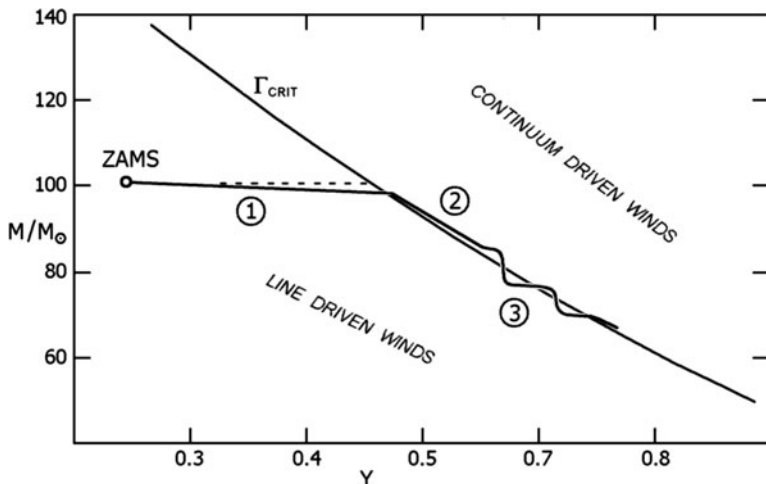


Fig. 12.5 Evolution of a very massive star: mass vs. helium fraction. (1) As long as a star is well below the Eddington limit, it will suffer only minor line driven mass-loss. (2) Once μ is large enough, the star exceeds the Eddington luminosity and loses mass rapidly. This forces the evolution to follow the Eddington luminosity from above. (3) Due to a yet unknown instability, excursions to high luminosities and mass-loss rates may occur with quiescent periods between. The *average* mass loss rate allows the star to follow L_{Edd} . Here we assume that $\Gamma_{\text{crit}} = 0.5$, but this number is actually unknown as it depends on the instabilities that cause atmospheres to become porous

But (12.7) also shows that a decrease in M tends to reduce the equilibrium luminosity; so we can reasonably expect $(\Gamma - 1)$ automatically to remain small. As μ continues to increase, the star moves downward along evolutionary stage 2 in Fig. 12.5, remaining near the Eddington limit. Eventually, unknown instabilities may cause the track to become unsteady like stage 3 in the figure. The example of η Car suggests that this may indeed be the case.

The evolution shown in Fig. 12.5 can continue as long as hydrogen is burning in the core, and very likely also after hydrogen is depleted. This is because similar constraints apply to the remaining WR star. The difference is that typical masses are smaller for helium stars, because μ is larger. Towards the end of hydrogen burning, the remaining mass will be typically much less than the ZAMS value.

12.5 Summary

The large mass loss rates observed in some LBVs, and especially in η -Carinae, strongly suggest that continuum driven winds play an important role. This is because continuum driving is the only mechanism known to give a steady state wind with a mass loss rate much larger than line driving can achieve.

A continuum-driven wind, however, can only operate in a system above the Eddington luminosity. This implies that such a star should have a rather unique structure. Its “static” part should be composed of a large convective region, encompassing most of the star, and a *porous* layer where inhomogeneities are responsible for a lowered opacity. At the radius where opacity cannot be sufficiently reduced by porosity, there is a transition between the gravitationally bound layer below and the radiatively accelerated wind above. Because the mass loss rate can be very large, the wind itself is optically thick so the photosphere resides within the wind.

Another peculiar aspect of continuum driven winds is that because the mass loss rate is determined from conditions at the “static” surface of the star, the wind conditions are blind to whether the available radiative luminosity is sufficient to actually drive the wind to infinity. If the potential well is too deep, the result is a *photon-tired wind*, whose flow stagnates and falls back.

Current 1-D simulation of photon-tired winds suggest that a flow of this type develops a layer with a hierarchical structure of shocks and sonically moving gas, which allows a large kinetic “luminosity” without driving mass above the photon-tired limit. It is not unreasonable that η Carinae actually reached this state, since the ejected mass divided by the 20 years of the giant eruption is, to within the rather large observational uncertainty, comparable to the photon-tired mass loss rate.

Although a super-Eddington state with a continuum-driven wind can be stationary on a dynamical timescale, the large mass loss rate should substantially alter the stellar structure on an evolutionary timescale. Stellar structure and evolution should effectively control the overall level of mass loss, implying that mass loss and evolution are inextricably linked. We thus expect very massive stars that reach the Eddington limit (which they do once the hydrogen mass fraction decreases sufficiently) to evolve with a luminosity that is kept slightly above the Eddington value, with a relatively modest continuum driven wind.

Perhaps the key unresolved questions concern the origin of variability in LBVs and their giant mass loss episodes. While there is a general understanding of how a super-Eddington state with the large mass loss can exist, there is yet no theory that predicts, for example, the two-decade-long giant eruption of η Car.

Acknowledgements S.P.O. acknowledges partial support from NSF and N.J.S. the support of ISF grant 1325/06. We thank J. MacDonald, N. Smith, R. Townsend, and A.J. van Marle for many helpful discussions.

References

1. I. Appenzeller, The role of radiation pressure in LBV atmospheres, in *Physics of Luminous Blue Variables*, ed. by K. Davidson et al. (Kluwer, Dordrecht, 1989), p. 195
2. J. Arons, Photon bubbles – overstability in a magnetized atmosphere. *ApJ*. **388**, 561 (1992)
3. G.T. Bath, G. Shaviv, Classical novae – a steady state, constant luminosity, continuous ejection model. *MNRAS*. **175**, 305 (1976)

4. M.C. Begelman, Super-eddington fluxes from thin accretion disks? *ApJ*. **568**, L97 (2002)
5. A.A. Belyanin, Optically thick super-Eddington winds in galactic superluminal sources. *A&A*. **344**, 199 (1999)
6. O. Blaes, A. Socrates, Local radiative hydrodynamic and magnetohydrodynamic instabilities in optically thick media. *ApJ*. **596**, 509 (2003)
7. J. Castor, D. Abbott, R. Klein, Radiation-driven winds in of stars. *ApJ*. **195**, 157 (1975)
8. K. Davidson, The relation between apparent temperature and mass-loss rate in Hypergiant Eruptions. *ApJ*. **317**, 760–764 (1987)
9. K. Davidson, Plinian Eruptions a la Eta Carinae, in *Physics of Luminous Blue Variables*, ed. by K. Davidson et al. (Kluwer, Dordrecht, 1989), p. 101
10. K. Davidson, in *Physics of Luminous Blue Variables*, ed. by K. Davidson et al. (Kluwer, Dordrecht, 1989), p. 203
11. K. Davidson, The physical nature of η Carinae, in *The Fate of the Most Massive Stars*, ed. by R. Humphreys, K. Stanek. ASP Conference Series, vol. 332 (Astronomical Society of the Pacific, San Francisco, 2005), pp. 101–110
12. K. Davidson, R.M. Humphreys, Eta Carinae and its environment. *Annu. Rev. Astron. Astrophys.* **35**, 1–32 (1997)
13. K. Davidson, N. Smith, T.R. Gull, K. Ishibashi, D.J. Hillier, The shape and orientation of the Homunculus nebula based on spectroscopic velocities. *AJ*. **121**, 1569–1577 (2001)
14. A.S. Eddington, *The Internal Constitution of the Stars*, Chapter 6. (Cambridge University Press, Cambridge, 1926)
15. D.F. Figer, An upper limit to the masses of stars. *Nature* **434**, 192 (2005)
16. C.F. Gammie, Photon bubbles in accretion discs. *MNRAS*. **297**, 929 (1998)
17. K. Gayley, An improved line-strength parameterization in hot-star winds. *ApJ*. **454**, 410 (1995)
18. W. Glatzel, On the origin of strange modes and the mechanism of related instabilities. *MNRAS*. **271**, 66 (1994)
19. W. Glatzel, M. Kiriakidis, Stability of massive stars and the Humphreys/Davidson limit. *MNRAS*. **263**, 375 (1993)
20. J.A. Guzik, Instability considerations for massive star Eruptions, in *The Fate of the Most Massive Stars*, ed. by R. Humphreys, K. Stanek. ASP Conference Series, vol. 332 (Astronomical Society of the Pacific, San Francisco, 2005), p. 204
21. J.A. Guzik, A.N. Cox, K.M. Despain, M.S. Soukup, A nonlinear study of LBVs and possible outbursts, in *Luminous Blue Variables: Massive Stars in Transition*, ed. by A. Nota, H. Lamers. ASP Conference Series, vol. 120 (Astronomical Society of the Pacific, San Francisco, 1997), p. 138
22. C.J. Hansen, S.D. Kawaler, V. Trimble, in *Stellar Interiors: Physical Principles, Structure, and Evolution*, 2nd edn., ed. by C.J. Hansen, S.D. Kawaler, V. Trimble (Springer-Verlag, New York, 2004)
23. R.M. Humphreys, K. Davidson, Studies of luminous stars in nearby galaxies. III – Comments on the evolution of the most massive stars in the milky way and the large Magellanic cloud. *ApJ*. **232**, 409 (1979)
24. R.M. Humphreys, K. Davidson, The most luminous stars. *Science* **223**, 243 (1984)
25. R.M. Humphreys, K. Davidson, The luminous blue variables: astrophysical geysers. *PASP*. **106**, 1025–1051 (1994)
26. R.M. Humphreys, K. Davidson, N. Smith, Crossing the yellow void: spatially resolved spectroscopy of the post-red supergiant IRC +10420 and its circumstellar ejecta. *AJ*. **124**, 1026 (2002)
27. P. Joss, E. Salpeter, J. Ostriker, On the “critical luminosity” in stellar interiors and stellar surface boundary conditions. *ApJ*. **181**, 429 (1973)
28. S.S. Kim, D.F. Figer, R.P. Kudritzki, F. Najarro, The arches cluster mass function. *ApJL*. **653**, L113 (2006)
29. H.J.G.L.M. Lamers, J.P. Cassinelli, *Introduction to Stellar Winds* (Cambridge University Press, Cambridge, 1999)

30. A. Maeder, On the evolutionary status and instability mechanism of the luminous blue variables, in *Physics of Luminous Blue Variables*, ed. by K. Davidson et al. (Kluwer, Dordrecht, 1989), p. 15
31. M.S. Oey, C.J. Clarke, Statistical confirmation of a stellar upper mass limit. *ApJL*. **620**, L43 (2005)
32. S. Owocki, K. Gayley, The physics of stellar winds near the Eddington limit, in *Luminous Blue Variables: Massive Stars in Transition*, ed. by A. Nota, H. Lamers. ASP Conference Series, vol. 120 (Astronomical Society of the Pacific, San Francisco, 1997), p. 121
33. S. Owocki, K. Gayley, N. Shaviv, A porosity-length formalism for photon-tiring-limited mass loss from stars above the Eddington limit. *ApJ*. **558**, 802 (2004)
34. J. Papaloizou, F. Albers, J.E. Pringle, G.J. Savonije, On the nature of strange modes in massive stars. *MNRAS*. **284**, 821 (1997)
35. T. Quinn, B. Paczynski, Stellar winds driven by super-Eddington luminosities. *ApJ*. **289**, 634 (1985)
36. G.J. Schwarz, P.H. Hauschildt, S. Starrfield, P.A. Whitelock, E. Baron, G. Sonneborn, A multiwavelength study of the early evolution of the classical Nova LMC 1988 1. *MNRAS*. **300**, 931 (1998)
37. N. Shaviv, The Eddington luminosity limit for multiphased media. *ApJ*. **494**, L193 (1998)
38. N. Shaviv, The porous atmosphere of N7 Carinae. *ApJ*. **532**, L137 (2000)
39. N. Shaviv, The nature of the radiative hydrodynamic instabilities in radiatively supported Thomson atmospheres. *ApJ*. **549**, 1093 (2001)
40. N. Shaviv, The theory of steady-state super-Eddington winds and its application to Novae. *MNRAS*. **326**, 126 (2001)
41. N. Shaviv, Exceeding the Eddington limit, in *The Fate of the Most Massive Stars*, ed. by R.M. Humphreys, K.Z. Stanek. ASP Conference Series, vol. 332 (Astronomical Society of the Pacific, San Francisco, 2005) pp. 180–188
42. N. Smith, S. Owocki, On the role of continuum-driven Eruptions in the evolution of very massive stars and population III stars. *ApJL*. **645**, 45 (2006)
43. N. Smith, R.D. Gehrz, P.M. Hinz, W.F. Hoffmann, J.L. Hora, E.E. Mamajek, M.R. Meyer, Mass and kinetic energy of the Homunculus Nebula around η Carinae. *AJ*. **125**, 1458–1466 (2003)
44. N. Smith, K. Davidson, T.R. Gull, K. Ishibashi, D.J. Hillier, Latitude-dependent effects in the stellar wind of eta Carinae. *ApJ*. **586**, 432–450 (2003)
45. V.V. Sobolev, *Moving Envelopes of Stars* (Harvard University Press, Cambridge, 1960)
46. E. Spiegel, Photohydrodynamic instabilities of hot stellar atmospheres, in *Physique des Mouvement dans les Atmospheres Stellaires*, ed. by R. Cayrel, M. Steinberg (CNRS, Paris, 1976) p. 19
47. E. Spiegel, Photoconvection, in *Problems in Stellar Convection*, ed. by E. Spiegel, J.-P. Zahn (Springer, Berlin, 1977), 267
48. E. Spiegel, L. Tao, Photofluid instabilities of hot stellar envelopes. *Phys. Rep.* **311**, 163 (1999)
49. R.B. Stothers, C.-W. Chin, On two theories of the cyclical outbursts of eta Carinae. *ApJ*. **489**, 319 (1997)
50. A.J. van Marle, S.P. Owocki, N. Shaviv, Continuum-driven winds from super-Eddington stars: a tale of two limits, in *First Stars III*, ed. by B.W. O'Shea, A. Heger, T. Abel, AIP Conference Proceedings, vol. 990 (American Institute of Physics, Melville, 2008), pp. 250–253
51. A.J. van Marle, S.P. Owocki, N. Shaviv, Numerical simulations of continuum-driven winds of super-Eddington stars. *MNRAS*. **389**, 1353 (2008)
52. C. Weidner, P. Kroupa, Evidence for a fundamental stellar upper mass limit from clustered star formation. *MNRAS*. **348**, 187 (2004)
53. S.E. Woosley, S. Blinnikov, A. Heger, Pulsational pair instability as an explanation for the most luminous supernovae. *Nature* **450**, 390 (2007)